

Contribution of electronic structure to thermoelectric power in $(\text{Bi,Pb})_2(\text{Sr,L a})_2\text{CuO}_{6+\delta}$

Takeshi Kondo,¹ Tsunehiro Takeuchi,² Uichiro Mizutani,¹ Takayoshi Yokoya,³ Syunsuke Tsuda,³ and Shik Shin³

¹*Department of Crystalline Materials Science, Nagoya University, Nagoya 464-8603, Japan*

²*Ecotopia Science Institute, Nagoya University, Nagoya 464-8603, Japan*

³*Institute of Solid State Physics, University of Tokyo, Kashiwa 277-8581, Japan*

(Received 24 August 2004; revised manuscript received 26 April 2005; published 20 July 2005)

The energy-momentum ($\varepsilon-\mathbf{k}$) dispersion and the shape of the Fermi surface in the $(\text{Bi,Pb})_2(\text{Sr,L a})_2\text{CuO}_{6+\delta}$ (Bi2201) superconductors with various hole concentrations were determined by the high resolution angle-resolved photoemission spectroscopy. On the basis of the $\varepsilon-\mathbf{k}$ dispersion thus obtained, temperature and hole-concentration dependence of the thermoelectric power $S(T)$ was calculated within the framework of the Boltzmann transport theory. $S(T)$ of the optimally and overdoped samples was quantitatively reproduced by the present calculation, strongly indicating that characteristics in $S(T)$ of the high- T_c cuprates under the optimally to overdoped conditions is unambiguously caused by the band structure characterized by the van Hove singularity near the Fermi level.

DOI: 10.1103/PhysRevB.72.024533

PACS number(s): 74.25.Fy, 74.72.Hs

I. INTRODUCTION

Thermoelectric power $S(T)$ of the high- T_c superconductors exhibits a unique temperature and hole-concentration (p) dependence.¹⁻⁶ $S(T)$ monotonically decreases with increasing p regardless of temperature. $S(T)$ in the optimally and underdoped samples shows strong temperature dependence described below, in sharp contrast to that in the overdoped samples staying negative and linearly decreasing with increasing temperature over a wide temperature range. The optimally and underdoped samples generally possess a positive value of $S(T)$ at low temperature. With increasing temperature, $S(T)$ at first increases and then starts to decrease after becoming maximal at T_{peak} . Above T_{peak} , $S(T)$ monotonically decreases with increasing temperature and eventually shows a negative value at $T \geq T_{\text{cross}}$. Both T_{peak} and T_{cross} decrease with increasing p . At high temperature above T_{cross} , $S(T)$ decreases linearly with increasing temperature. The characteristic behavior of $S(T)$ observed for the optimally and underdoped samples is definitely inconsistent with the T -linear dependence, which is generally observed in typical metallic phases and is usually given by

$$S(T) = \frac{\pi^2 k_B T}{-3|e|} \left[\frac{\partial \ln \sigma(\varepsilon)}{\partial \varepsilon} \right]_{\varepsilon=\mu}, \quad (1)$$

where $\sigma(\varepsilon)$ is the spectral conductivity.

Obertelli *et al.*⁷ pointed out that the $S(290 \text{ K})$ in a number of cuprate superconductors drops on a “universal” curve when it is plotted as a function of T_c/T_c^{max} . They suggested, as a consequence of the $S(290 \text{ K})$ vs T_c/T_c^{max} plot, that the value of $S(290 \text{ K})$ can be used as a measure for the p by additionally employing an empirical relation $T_c/T_c^{\text{max}} = 1 - 82.6(p - 0.16)^2$ reported by Presland *et al.*⁸ Although physical interpretation of the relation between $S(290 \text{ K})$ and T_c/T_c^{max} has not been well established, $S(290 \text{ K})$ has been often used to estimate unknown “ p ” in the high- T_c cuprates according to the Obertelli’s relation.

Note that the Obertelli’s “universal” relation between $S(290 \text{ K})$ and p was reported invalid for some superconductors such as $\text{La}_{2-x}\text{Sr}_x\text{CuO}_4$ (LSCO)^{1,9,10} and $\text{Bi}_2\text{Sr}_{2-z}\text{La}_z\text{CuO}_{6+\delta}$ (La-doped Bi2201).¹¹ It is, therefore, strongly required to confirm the validity of the relation between $S(290 \text{ K})$ and p by investigating the mechanism inducing the characteristic behavior of $S(T)$ in the cuprate superconductors. Since the “universal” relation between $S(290 \text{ K})$ and p is constructed on the basis of the two empirical relations, $S(290 \text{ K})$ vs T_c/T_c^{max} and T_c/T_c^{max} vs p , the validity of both relations has to be carefully investigated.

Several attempts had already been made to account for the characteristic behaviors of $S(T)$ in the cuprates superconductors.^{9,12-18} Some of these studies are conducted on the basis of a pure charge-carrier diffusion mechanism, including the narrow-band effects.^{9,16-18} McIntosh and Kaiser¹⁸ used a hypothetical band structure to estimate $S(T)$, and succeeded in qualitatively accounting for the behavior of the $S(T)$ in terms of the presence of van Hove singularity (vHs) inherent in the two-dimensional system. Although the electronic structure employed by McIntosh and Kaiser was certainly different from the real one, which is revealed by a large number of angle-resolved photoemission (ARPES) studies, the presence of vHs near the chemical potential is indeed one of the most characteristic properties in the electronic structure of the high- T_c superconductors.¹⁹⁻²³ It is, thus, strongly expected that if a precisely determined electronic structure is employed instead of the hypothetical one, the calculated $S(T)$ would quantitatively reproduce the measured data.

ARPES is widely known as a unique and powerful experimental technique to study the momentum-resolved electronic structure. Recent development of the energy and momentum resolutions in the ARPES measurement allows us to quantitatively discuss the electronic transport properties by using the ARPES spectra. In this work, we employed ARPES measurements for the $(\text{Bi,Pb})_2(\text{Sr,L a})_2\text{CuO}_{6+\delta}$ (Bi2201) single crystals with various p ’s to interpret their characteristic behaviors of $S(T)$.

TABLE I. Sample preparation conditions for the present Bi2201 single crystals.

Nominal composition	Atmosphere	Temperature	T_c	Label
(Bi _{1.74} Pb _{0.38})Sr _{1.88} CuO _{6+δ}	2 atm O ₂	400 °C for 72 h	<2 K	OD0K
(Bi _{1.74} Pb _{0.38})Sr _{1.88} CuO _{6+δ}	1 atm Air	750 °C for 24 h	7 K	OD7K
(Bi _{1.74} Pb _{0.38})Sr _{1.88} CuO _{6+δ}	Vacuum	650 °C for 24 h	21 K	OD21K
(Bi _{1.35} Pb _{0.85})(Sr _{1.47} La _{0.38})CuO _{6+δ}	Ar flow	650 °C for 24 h	35 K	OP35K
(Bi _{1.35} Pb _{0.85})(Sr _{1.40} La _{0.45})CuO _{6+δ}	Ar flow	650 °C for 24 h	27 K	UD27K

We selected the Pb-substituted Bi2201, which is a single-layered cuprate free from the structure modulation, because it possesses only one band crossing the Fermi level^{19,24} in sharp contrast to the complicated electronic structure in the Bi₂Sr₂CaCu₂O_{8+ δ} (Bi2212) characterized by the bilayer splitting^{25–27} and Umklapp-bands^{28,29} caused by the incommensurate structure modulation in the Bi-O layers. Their low critical temperature $T_c^{\max} \approx 35$ K and ability in wide range carrier-doping further encouraged us to employ the Bi2201 samples for the investigation of normal state properties by using the ARPES spectra.

The band structure (the ε - \mathbf{k} dispersion) was precisely determined from the measured ARPES spectra. $S(T)$ of these samples was calculated within the framework of the Boltzmann transport theory on the basis of the experimentally determined ε - \mathbf{k} dispersion. By comparing the calculated $S(T)$ with the measured one, we demonstrate that it is inappropriate to use Obertelli's relation for estimating p .

II. EXPERIMENTAL PROCEDURE

(Bi,Pb)₂(Sr,La)₂CuO_{6+ δ} (Bi2201) single crystals were grown by the conventional floating-zone (FZ) technique. Synthesized crystals were cut into typically (1–3) × 3 × 0.05 mm in dimension. The partial substitution of Pb for Bi removes the superstructure along the b axis,^{24,30–32} that is one of the most famous structural features in the Bi-based superconductors and has prevented us from easily analyzing the band structure by inducing unfavorable Umklapp bands.^{29,33} Hole concentration, p , was controlled by the partial substitution of La for Sr and the subsequent heat treatments. The partial substitution of La for Sr is needed to reduce the doping level from the optimally to the underdoped condition, while the La-free Bi2201 samples yield in the overdoped condition in which p can be widely controlled simply by the annealing. The nominal compositions and the annealing conditions are summarized in Table I together with the resulting T_c .

T_c of each sample was determined by the dc susceptibility measurement and the electrical resistivity measurement. The thermoelectric power $S(T)$ of these samples was measured in the temperature range from 90 to 400 K with the Seebeck Coefficient Measurement System, MMR inc.

The overdoped samples of $T_c < 2$ K, $T_c = 7$ K, and $T_c = 21$ K were labeled as OD0K, OD7K, and OD21K, respectively. The OD0K possesses no evidence for the superconductivity in its dc susceptibility nor in the electrical resistivity at temperatures above 2 K. The optimally doped sample

of $T_c = 35$ K and the underdoped sample of $T_c = 27$ K were labeled as OP35K and UD27K, respectively.

High-resolution ARPES spectra were accumulated using the Scienta SES2002 hemispherical analyzer with the Gammatdata VUV5010 photon source (HeI α) at the Institute of Solid State Physics (ISSP), the University of Tokyo. The angular and energy resolutions employed in this work were 0.13° and 10 meV, respectively. The ε - \mathbf{k} dispersion in an energy range of a few $k_B T$ across the chemical potential μ has to be investigated for the quantitative evaluation of the temperature dependence of the electronic transport properties. Although it is often argued that the photoemission spectroscopy measurement cannot reveal the unoccupied part of the electronic states above μ , we have to stress here that it does probe the conduction band even though the energy range is restricted in a very narrow energy range up to a few $k_B T$ above μ because of the nonzero value of the Fermi-Dirac distribution function (FD(ε, T)) in this particular energy range. In this study, we intentionally measured the spectra at 200 K rather than at low temperature to obtain the band structure both above and below μ . Moreover, by dividing the measured spectra by FD($\varepsilon, 200$ K), we obtained the ε - \mathbf{k} dispersion up to ~ 50 meV above μ , as clear as that below μ .^{24,34}

III. RESULTS

A. Thermoelectric power

The measured $S(T)$'s of OD0K, OD7K, OD21K, OP35K, and UD27K are shown in Fig. 1. Obviously, $S(T)$ of the present Bi2201 samples possesses a strong p dependence; $S(T)$ in the overdoped samples stays negative and decreases almost linearly with increasing temperature over the whole temperature range of the measurement. On the other hand, $S(T)$ in the optimally and underdoped samples possesses a positive value at low temperature and increases with increasing temperature below T_{peak} . Then $S(T)$ starts to decrease, and eventually reaches below zero at T_{cross} . The same characteristics were generally observed in other cuprate superconductors.^{1–6} The additional characteristics in $S(T)$ can be also stressed in the heavily overdoped samples. $S(T)$ in the OD0K sample, which is expected to be nearly “normal metal,” possesses weak nonlinear temperature dependence. This experimental fact cannot be explained by Eq. (1), though Eq. (1) is frequently used to evaluate $S(T)$ of the metallic compounds.

Figure 2 shows T_c/T_c^{\max} of the present Bi2201 plotted as a function of $S(290$ K) together with the data previously re-

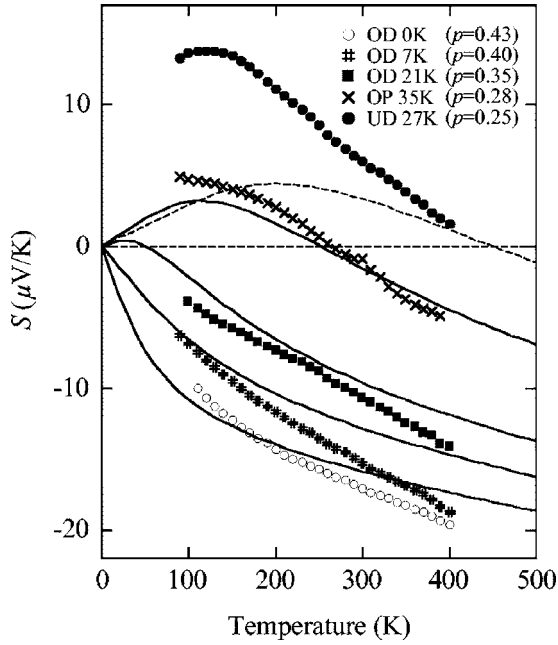


FIG. 1. The measured and calculated $S(T)$ of OD0K, OD7K, OD21K, OP35K, and UD27K. The calculated $S(T)$ are shown by the solid lines for OD0K, OD7K, OD21K, and OP35K, and by a dashed line for UD27K. The quantitative agreement is observed for the optimally and overdoped samples. The calculated $S(T)$ of UD27K deviates from the measured one, particularly at a low temperature.

ported for other cuprates.^{1,3-6,11} The “universal” curve of T_c/T_c^{\max} vs $S(290\text{ K})$, proposed by Obertelli *et al.*,⁷ is superimposed by the dashed line in Fig. 2. Although it shows appropriate consistency at negative $S(290\text{ K})$, the relation between T_c/T_c^{\max} and $S(290\text{ K})$ for the Bi2201, including

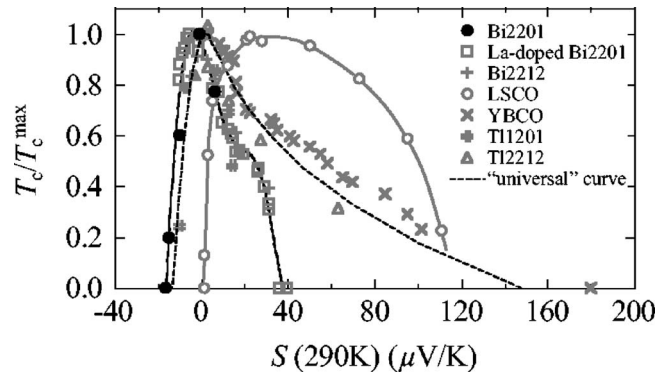


FIG. 2. T_c/T_c^{\max} as a function of $S(290\text{ K})$ in the present (Bi,Pb)₂(Sr,La)₂CuO_{6+δ} (Bi2201). The data for various high- T_c cuprates of Bi₂Sr_{2-z}La_zCuO_{6+δ} (La-doped Bi2201) (Ref. 11), Bi₂Sr₂Ca_{1-x}Nd_xCu₂O_y (Bi2212) (Ref. 3), La_{2-x}Sr_xCuO₄ (LSCO) (Ref. 1), YBa₂Cu₃O_y (YBCO) (Ref. 4), Tl_{0.5}Pb_{0.5}Sr_{2-x}La_xCuO₅ (Tl1201) (Ref. 5), and Tl₂Ba₂Ca_{1-x}Y_xCu₂O_{8+y} (Tl2212) (Ref. 6), are superimposed. The “universal” curve proposed by Obertelli *et al.* (Ref. 7) is shown by the dashed line. The solid lines are drawn for the guide to the eye, which clearly show that T_c/T_c^{\max} vs $S(290\text{ K})$ in Bi2201, La-doped Bi2201 and LSCO obviously possess data far from the “universal” curve.

our present samples, obviously deviates from the “universal” curve. This deviation was more pronounced for LSCO.¹ These experimental facts strongly indicate that the “universal” curve proposed by Obertelli *et al.*⁷ may not be universally valid.

B. Band structure determined by ARPES

The electronic structure of cuprate superconductors has already been frequently studied, and it is already known as a consequence of these studies that the shape of the FS in the Bi2201 is slightly different from that in Bi2212 or LSCO.^{20,22,35} It is, therefore, strongly expected that the difference in the T_c/T_c^{\max} vs $S(290\text{ K})$ curve among the various cuprates is caused by the difference in the band structure, which leads to the difference in the FS shape. In order to quantitatively evaluate the role of the band structure that is responsible for the characteristic temperature and p dependence in $S(T)$, the band structure about μ was precisely determined by the present ARPES measurement.

Figures 3(a-A), (a-B), and (a-C) show momentum- and energy-dependent ARPES intensity at 200 K, $\text{Int}(\epsilon, \mathbf{k}, 200\text{ K})$, for the OD0K measured along momentum lines A, B, and C, respectively, shown in Fig. 3(e). It is obviously confirmed in Figs. 3 (a-A)–(a-C) that the $\text{Int}(\epsilon, \mathbf{k}, 200\text{ K})$ has small but finite intensity even above μ due to the thermal excitation. The measured $\text{Int}(\epsilon, \mathbf{k}, 200\text{ K})$'s along three \mathbf{k} lines of A–C were divided by the $\text{FD}(\epsilon, 200\text{ K})$ and shown in Figs. 3 (b-A)–(b-C). The $\epsilon - \mathbf{k}$ dispersion above μ is much more clearly observed in $\text{Int}(\epsilon, \mathbf{k}, 200\text{ K})/\text{FD}(\epsilon, 200\text{ K})$ than that in $\text{Int}(\epsilon, \mathbf{k}, 200\text{ K})$.

By extracting energy distribution curves (EDC's) and momentum distribution curves (MDC's) from $\text{Int}(\epsilon, \mathbf{k}, 200\text{ K})/\text{FD}(\epsilon, 200\text{ K})$ and taking the peak energy ($\epsilon_{\text{EDC}}(k_x, k_y)$) and the peak momentum ($\epsilon_{\text{MDC}}(k_x, k_y)$) of these EDC's and MDC's, the $\epsilon - \mathbf{k}$ dispersion was successfully determined in the energy range of $-300 \leq \epsilon \leq 50\text{ meV}$ for OD0K, OD7K, OD21K, OP35K, and UD27K. For example, extracted MDC and EDC with the fitting curve of a Lorentzian shape are shown in Figs. 3(c) and 3(d), respectively. A large number of data points of $\epsilon(k_x, k_y)$ in the OD7K thus determined by the ARPES measurement is shown in Fig. 4 as a typical example.

Note here that $\epsilon_{\text{MDC}}(k_x, k_y)$ is not exactly the same with $\epsilon_{\text{EDC}}(k_x, k_y)$, which directly represents the eigenvalue of electrons ($\epsilon(k_x, k_y)$), at high binding energies. This inconsistency is brought about by the nonsymmetrical shape of the spectral function appearing in EDC's and pronounced at high binding energies. In the narrow energy range of $-50 \leq \epsilon \leq 50\text{ meV}$, this inconsistency between $\epsilon_{\text{MDC}}(k_x, k_y)$ and $\epsilon_{\text{EDC}}(k_x, k_y)$ is not seriously obvious, and hence we mainly used MDC's having a symmetrical Lorentzian shape to easily determine the precise $\epsilon(k_x, k_y)$ rather than using EDC's having a complicated line shape. EDC's were used to determine $\epsilon(k_x, k_y)$ below $\epsilon = -50\text{ meV}$, where the error in $\epsilon_{\text{MDC}}(k_x, k_y)$ is enhanced. Although it is located near μ , $\epsilon(k_x, k_y)$ about the $(\pi, 0)$ point was also determined from $\epsilon_{\text{EDC}}(k_x, k_y)$ because it was difficult to separate two peaks overlapped in MDC.

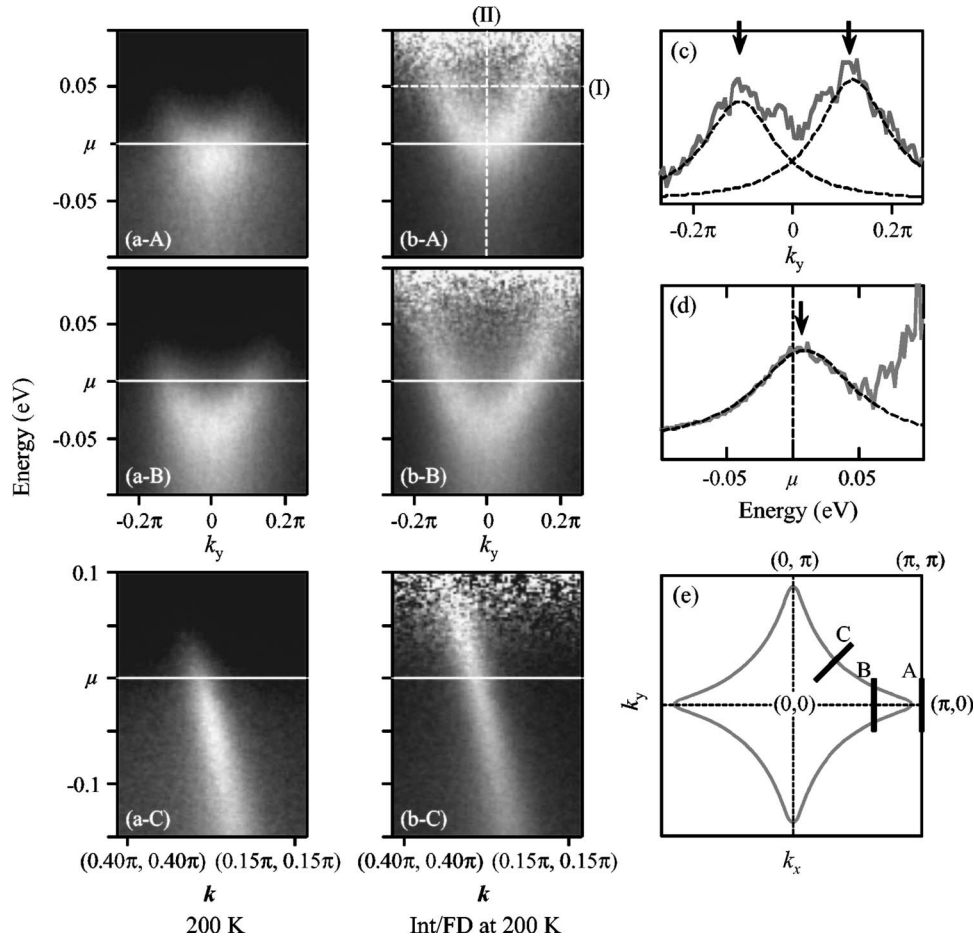


FIG. 3. (a) The ARPES intensity images of OD0K measured at 200 K, $\text{Int}(\varepsilon, \mathbf{k}, 200 \text{ K})$. A, B, and C refer to the measured momentum lines in the first Brillouin Zone shown in (e). Thermal broadening is observed for up to a few $k_B T$ above μ . (b) $\text{Int}(\varepsilon, \mathbf{k}, 200 \text{ K})$ divided by the Fermi-Dirac distribution function at 200 K. The ε - \mathbf{k} dispersion up to a few $k_B T$ above μ can be more clearly observed. (c) MDC measured at the energy shown by a dashed line (I) in (b-A), and (d) EDC measured along the dashed line (II) in (b-A). Momentum and energy of the peaks in MDC and EDC were determined by the Lorentzian-function fitting.

It is found that the fairly large van Hove singularity (vHs) persists at the $(\pi, 0)$ point regardless of the hole concentration. This vHs is generally observed near μ in all cuprates superconductors. The energy of the vHs (ε_{vHs}) increases with increasing hole concentration, and eventually exceeds μ in the OD0K of the highest hole concentration among those in the present samples; ε_{vHs} 's of OD0K, OD7K, OD21K, OP35K, and UD27K are -4 , 6 , 16 , 42 , and 70 meV, respectively. The negative value of ε_{vHs} only for OD0K is consistent with the result reported by Takeuchi *et al.*,¹⁹ who claimed that the $\varepsilon(\pi, 0)$ of OD0K is located above μ . Thus, we stress here that only the heavily overdoped Bi2201 with a T_c of less than 2 K has an electronlike Fermi surface (FS) centered at the $(0, 0)$ point, while all other samples with a smaller hole concentration show the holelike FS centered at the (π, π) point.

We reported in our previous work that the ε - \mathbf{k} dispersion is kept almost rigid over a wide hole concentration range from the optimally to overdoped condition.³⁵ In the present study, the rigid band is also confirmed in the lightly underdoped sample of UD27K. Thus we decided to use the $\varepsilon(k_x, k_y)$ of OD7K, shown in Fig. 4, to evaluate $S(T)$ in all

samples with shifting μ so as the resulting ε_{vHs} coincide with the measured value.

We employed here the tight-binding fitting method on the experimentally determined $\varepsilon(k_x, k_y)$ for OD7K, which discretely scatter in the reciprocal space, as shown in Fig. 4. Six tight-binding functions²⁰ employed in this study are listed in Table II together with the obtained coefficients. Although it has to be used for the tight-binding fitting, the eigenvalue at

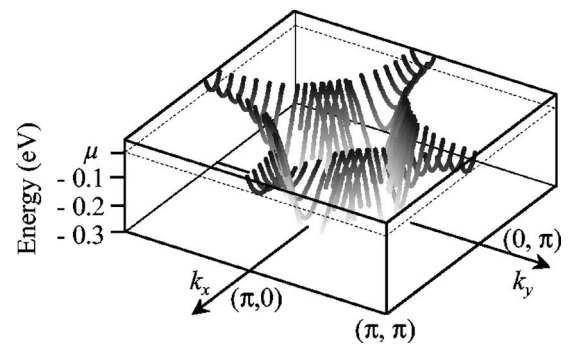


FIG. 4. The ε - \mathbf{k} dispersion determined from the peaks in the ARPES spectra for OD7K.

TABLE II. Fitting functions and resulting coefficients in the present tight-binding fit on the experimentally determined dataset of $\varepsilon(k_x, k_y)$ for OD7K.

i	n_i	t_i (eV)
0	1	0.2716
1	$1/2(\cos k_x + \cos k_y)$	-0.8528
2	$\cos k_x \cos k_y$	0.1772
3	$1/2(\cos 2k_x + \cos 2k_y)$	-0.1574
4	$1/2(\cos 2k_x \cos k_y + \cos k_x \cos 2k_y)$	-0.0828
5	$\cos 2k_x \cos 2k_y$	0.0571

the (π, π) point, $\varepsilon(\pi, \pi)$, cannot be experimentally determined because it stays far above μ . We tentatively employed 1.3 eV as the $\varepsilon(\pi, \pi)$ for OD7K. This value is very close to that used by Norman *et al.*²⁰ for the optimally doped Bi2212. Even though we used a less precise value for $\varepsilon(\pi, \pi)$, the resulting $\varepsilon(k_x, k_y)$ near μ obtained by the tight-binding method is reliable because a large number of data points in this particular energy range were precisely determined by the ARPES measurement and used for the fitting.

We have to comment on the effect of the mass renormalization caused by a bosonic collective mode in the energy scale of 40–70 meV,^{36,37} because this effect is not rigorously taken into account in our present analysis. It is well known that the mass-renormalization effect causes the smaller group velocity $\sim v/\alpha$ and the larger density of states $\sim \alpha N(\varepsilon)$. Since the spectral conductivity $\sigma(\varepsilon)$ that determines $S(T)$ is proportional to the product of the group velocity and the density of states, the resulting spectral conductivity is not affected by the mass renormalization. We, therefore, strongly believe that the $S(T)$ is not greatly modified, even under the influence of the bosonic mode, and that the present analysis would lead to the proper understanding about the role of the electronic structure to the characteristic behaviors in $S(T)$.

From the ε - \mathbf{k} dispersion thus determined, we calculated the electronic density of states $N(\varepsilon)$. The resulting $N(\varepsilon)$ for OP35K is shown in Fig. 5 together with that of the optimally doped Bi2212, which is calculated from the ε - \mathbf{k} dispersion

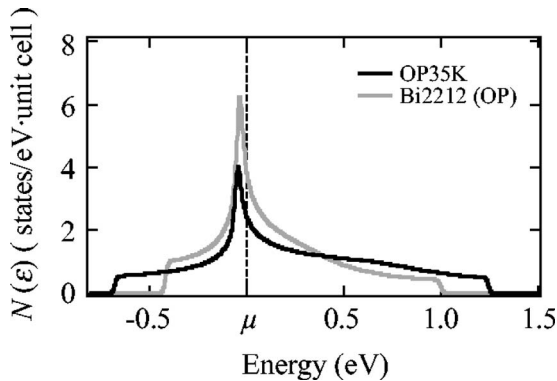


FIG. 5. The density of states $N(\varepsilon)$ of OP35K calculated from the ε - \mathbf{k} dispersion determined by the ARPES measurement. $N(\varepsilon)$ of optimally doped Bi2212 calculated from the ε - \mathbf{k} dispersion reported by Norman *et al.* (Ref. 20) is superimposed.

reported by Norman *et al.*²⁰ The $N(\varepsilon)$ of the present Bi2201 is characterized by the less significant vHs than that in Bi2212. This difference indicates that the flat ε - \mathbf{k} dispersion of the saddle point observed at $(\pi, 0)$ is more extended in Bi2212 than in Bi2201.

Hole concentration p was calculated from the area surrounded by the holelike FS centered at (π, π) , A_{pFS} , by using the relation of $p=2(A_{\text{pFS}}/A_{\text{BZ}})-1$, where A_{BZ} indicates the area of the first Brillouin zone (BZ). The shape of FS for these samples was reported in detail elsewhere.³⁵ The A_{pFS} 's in the OD0K, OD7K, OD21K, OP35K, and UD27K were determined to be 72%, 70%, 67%, 64%, and 62% of A_{BZ} , respectively. Thus the resulting p 's for OD0K, OD7K, OD21K, OP35K, and UD27K yield 0.43, 0.40, 0.35, 0.28, and 0.25 holes/Cu, respectively.

It has been argued that p in the high- T_c superconducting phase extends from ~ 0.05 to ~ 0.3 holes/Cu. This argument is based on the p in LSCO, that is unambiguously determined from its stoichiometric composition.^{38,39} The empirical relation $T_c/T_c^{\text{max}}=1-82.6(p-0.16)^2$ was proposed on the basis of the relation between T_c/T_c^{max} and p in LSCO.⁸ We have confirmed by using reported FS' determined by the ARPES measurement that p in Bi2212⁴⁰ and LSCO²² indeed falls into this particular range. However, the present Bi2201 samples obviously have a much larger p , ranging from 0.25 to 0.43 holes/Cu. This experimental fact suggests that the hole-concentration range of $0.05 < p < 0.3$ holes/Cu for the high- T_c superconductors and the relation of $T_c/T_c^{\text{max}}=1-82.6(p-0.16)^2$ cannot be used, at least in our present Bi2201 samples.

IV. DISCUSSION

In this section, the thermoelectric power $S(T)$ of Bi2201 is discussed in terms of the electronic structure near μ , determined by the present ARPES measurement.

The $S(T)$ of metallic phases is, in general, believed to possess T -linear dependence according to Eq. (1). However, the nonlinear temperature dependence in $S(T)$ suggests that we cannot use Eq. (1) for the present Bi2201. We introduce here the more rigorous equation from which Eq. (1) is deduced:

$$S(T) = \frac{1}{|e|T} \frac{\int_{-\infty}^{\infty} \sigma(\varepsilon)(\varepsilon - \mu) \left(\frac{\partial f(\varepsilon)}{\partial \varepsilon} \right) d\varepsilon}{\int_{-\infty}^{\infty} \sigma(\varepsilon) \left(-\frac{\partial f(\varepsilon)}{\partial \varepsilon} \right) d\varepsilon}. \quad (2)$$

Here $\sigma(\varepsilon)$ and $f(\varepsilon)$ represent the spectral conductivity and the Fermi-Dirac distribution function, respectively. For the transformation from Eq. (2) to Eq. (1), $\sigma(\varepsilon)$ is assumed to vary linearly with energy in the narrow energy window in which $(-\partial f(\varepsilon)/\partial \varepsilon)$ has a nontrivial value. As shown in Fig. 5, the density of states $N(\varepsilon)$ in high- T_c cuprates is characterized by the presence of vHs near μ , and does possess a nonlinear energy dependence within this narrow energy window. It is, thus, expected that $\sigma(\varepsilon)$ also possesses a nonlinear energy dependence and that Eq. (1) is no longer valid to estimate $S(T)$ of the high- T_c cuprates.

McIntosh and Kaiser¹⁸ calculated $S(T)$ of the cuprates by using Eq. (2) and the hypothetical $\sigma(\varepsilon)$. Their $\sigma(\varepsilon)$ consists of two components from narrow and wide two-dimensional bands. The former provides large vHs near μ and the latter linearly increasing $N(\varepsilon)$ with increasing energy. Their calculated $S(T)$ qualitatively accounted for the observed $S(T)$ in the cuprates without assuming any special scattering mechanism for the conduction electrons. However, the two-band electronic structure, which was indispensable to reproduce the measured $S(T)$ in their calculation, is not experimentally observed in Bi2201, but the one-band structure crossing the Fermi level is unambiguously observed by the ARPES measurement. Since we have precisely determined the electronic structure of Bi2201, it is now a good opportunity to verify the scenario of the vHs-inducing unusual thermopower using the experimentally determined electronic structure. The calculation of $S(T)$ with the experimentally determined electronic structure is the first attempt and should provide new and important information about the nature of high- T_c cuprates.

Here we employ the Boltzmann transport equation to calculate $\sigma(\varepsilon)$;

$$\sigma(\varepsilon) = \frac{e^2}{V} \sum_{\mathbf{k}} v_{\alpha}(\varepsilon, \mathbf{k}) l_{\alpha}(\varepsilon, \mathbf{k}) \delta[\varepsilon(\mathbf{k}) - \varepsilon], \quad (3)$$

where $l_{\alpha}(\varepsilon, \mathbf{k})$ and $v_{\alpha}(\varepsilon, \mathbf{k})$ ($\alpha=x$ or y) represent the mean-free path and the group velocity of the conduction electron at an eigenstate $(\varepsilon, \mathbf{k})$, respectively. The mean-free path $l_{\alpha}(\varepsilon, \mathbf{k})$ is described as

$$l_{\alpha}(\varepsilon, \mathbf{k}) \equiv v_{\alpha}(\varepsilon, \mathbf{k}) \cdot \tau(\varepsilon, \mathbf{k}), \quad (4)$$

where $\tau(\varepsilon, \mathbf{k})$ represents the relaxation time.

The scattering probability of the electron in the eigenstate of $(\varepsilon, \mathbf{k})$ is proportional to the energy width of the EDC spectrum. If the EDC spectrum has a symmetrical shape, l_{α} can be estimated from the peak width of MDC (Δk_{α}) with the relation of $l_{\alpha} \approx 1/\Delta k_{\alpha}$.⁴¹ This condition takes place in the vicinity of E_F , at which the energy-window function $(-\partial f(\varepsilon)/\partial \varepsilon)$ restricts the integration in Eq. (2). This means that the relation of $l_{\alpha} \approx 1/\Delta k_{\alpha}$ can be used to estimate the mean-free path l_{α} in our present analysis. We observed a nearly direction-independent peak width of MDC at E_F in the overdoped sample, which suggests that the scattering events in the overdoped sample are nearly direction independent. In addition, the width of MDC was kept almost constant within the energy range of $-50 \leq \varepsilon \leq 50$ meV centered at μ in the overdoped sample, strongly indicating that the mean-free path is almost energy independent in the narrow energy range. Therefore we assumed an energy- and momentum-independent l_{α} to calculate $S(T)$. As a consequence, l_{α} comes out from integrals both in numerator and denominator of Eq. (2) and is canceled out.

The $\sigma(\varepsilon)$ for OP35K evaluated from the experimentally determined ε - \mathbf{k} dispersion under the assumption of constant l_{α} is shown in Fig. 6(a). A hump in the $\sigma(\varepsilon)$ located near μ is caused by the presence of vHs in $N(\varepsilon)$, as shown in Fig. 5. One may wonder that the hump in the $\sigma(\varepsilon)$ should be as

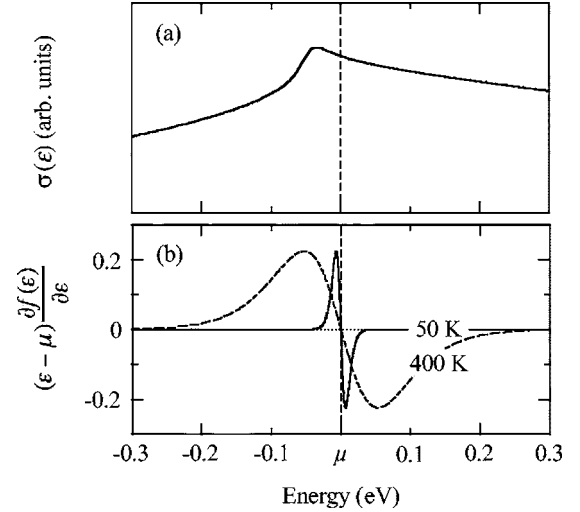


FIG. 6. (a) $\sigma(\varepsilon)$ for OP35K calculated from the ε - \mathbf{k} dispersion determined by the ARPES measurement within the framework of the Boltzmann transport theory under an assumption of constant l . (b) $(\varepsilon - \mu)(\partial f(\varepsilon)/\partial \varepsilon)$ at 50 and 400 K.

strong as vHs in the $N(\varepsilon)$. We should comment that even though their contribution to the $N(\varepsilon)$ is fairly pronounced, the electrons associated with vHs have small $v(\varepsilon, \mathbf{k})$ to provide a less significant contribution to the $\sigma(\varepsilon)$. A less-pronounced effect of the vHs on $\sigma(\varepsilon)$ due to the small group velocity was not taken into account in the McIntosh and Kaiser analysis, therefore, which overestimated the effect of vHs on $S(T)$.

We calculated $S(T)$ using Eq. (2) with $\sigma(\varepsilon)$ shown in Fig. 6(a). Here the Fermi level was shifted by the energy in the calculation of $S(T)$ in OD0K, OD7K, OD21K, OP35K, and UD27K according to the doping level of each sample so ε_{vHs} coincides with the measured value. The resulting $S(T)$ is superimposed on the measured one in Fig. 1. The calculated $S(T)$ quantitatively reproduces the measured one for the optimally and overdoped samples, while only the $S(T)$ of UD27K is not quantitatively reproduced by the present calculation. The fairly good agreement between the calculated $S(T)$ and the measured one in the optimally and overdoped samples suggests that the temperature and p dependence of $S(T)$ in high- T_c cuprates in these doping conditions is simply caused by the topology of electronic structure characterized by the presence of vHs near μ rather than by the strong electron correlation. These results encourage us to believe that the effect of the electron correlation does not contribute to induce the unusual behavior of $S(T)$ in optimally and overdoped samples of all cuprates superconductors, but only those in the underdoped samples. The threshold, where our calculation of $S(T)$ becomes invalid, was unambiguously determined to be near the optimally doped condition.

Before discussing the reason for the inconsistency between the measured and calculated $S(T)$ in the underdoped sample, we discuss here the mechanism leading to the characteristic behaviors of $S(T)$ of the cuprate superconductors in the optimally and overdoped conditions.

$S(T)$ can be easily understood by dividing Eq. (2) into three different quantities: $Q_+(T)$, $Q_-(T)$, and $\sigma(T)$ given by

$$Q_+(T) = \frac{1}{|e|} \int_{-\infty}^{\mu} \sigma(\varepsilon)(\varepsilon - \mu) \frac{\partial f(\varepsilon)}{\partial \varepsilon} d\varepsilon, \quad (5)$$

$$Q_-(T) = \frac{1}{|e|} \int_{\mu}^{\infty} \sigma(\varepsilon)(\varepsilon - \mu) \frac{\partial f(\varepsilon)}{\partial \varepsilon} d\varepsilon, \quad (6)$$

and

$$\sigma(T) = \int_{-\infty}^{\infty} \sigma(\varepsilon) \left(-\frac{\partial f(\varepsilon)}{\partial \varepsilon} \right) d\varepsilon, \quad (7)$$

respectively. $S(T)$ is expressed as $S(T) = (|Q_+(T)| - |Q_-(T)|) / (T\sigma(T))$.

Electrical conductivity $\sigma(T)$ can be considered as the average value of $\sigma(\varepsilon)$ within the energy window of $(-\partial f(\varepsilon)/\partial \varepsilon)$, because the function $(-\partial f(\varepsilon)/\partial \varepsilon)$ has a Gaussian-like shape and its integrated intensity $\int_{-\infty}^{\infty} (-\partial f(\varepsilon)/\partial \varepsilon) d\varepsilon$ provides unity regardless of the temperature. Since the averaged $\sigma(\varepsilon)$ over an energy range of a few $k_B T$ centered at μ does not drastically vary with varying temperature, especially in the present calculation, under the assumption of the constant l_{av} , $(|Q_+(T)| - |Q_-(T)|) / T$ mainly contributes the characteristic behaviors of $S(T)$.

$Q_+(T)$ and $Q_-(T)$ are obtained by the integration of the $\sigma(\varepsilon)$ multiplied by $(\varepsilon - \mu)(\partial f(\varepsilon)/\partial \varepsilon)$ in the energy range below and above μ , respectively. Their temperature dependence would be easily understood, if $\sigma(\varepsilon)$ and T dependence of $(\varepsilon - \mu)(\partial f(\varepsilon)/\partial \varepsilon)$ are separately treated. In Fig. 6, $(\varepsilon - \mu) \times (\partial f(\varepsilon)/\partial \varepsilon)$ at 50 and 400 K are represented, together with $\sigma(\varepsilon)$, for OP35K. The function $(\varepsilon - \mu)(\partial f(\varepsilon)/\partial \varepsilon)$ has a positive value below μ and a negative value above μ . The positive and negative peaks in the $(\varepsilon - \mu)(\partial f(\varepsilon)/\partial \varepsilon)$, located at $\varepsilon \approx \pm 1.3k_B T$, shift to lower and higher energy with increasing temperature, respectively. Thus, the difference between $\sigma(\varepsilon)$ about $\varepsilon = -1.3k_B T$ and that about $\varepsilon = +1.3k_B T$ would have an important role to determine $S(T)$.

The $|Q_+(T)|/T$ and $|Q_-(T)|/T$ of OP35K are calculated as a function of temperature and shown in Fig. 7. Since $\sigma(\varepsilon)$ has a negative slope near μ , $\sigma(-1.3k_B T)$ is larger than $\sigma(+1.3k_B T)$ at a low temperature and the difference increases with increasing temperature. This condition leads to larger $|Q_+(T)|/T$ than $|Q_-(T)|/T$, and the resulting $(|Q_+(T)| - |Q_-(T)|) / T$ continuously increases with increasing temperature. Once the temperature is increased as far as the positive peak of $(\varepsilon - \mu)(\partial f(\varepsilon)/\partial \varepsilon)$ reaches the energy of the hump in $\sigma(\varepsilon)$, $|Q_+(T)|/T$ starts to rapidly decrease with increasing temperature. Thus $S(T)$ shows a maximum at a particular temperature T_{peak} .

At a high temperature, the hump in $\sigma(\varepsilon)$ has a less significant contribution to $S(T)$ because the positive and negative peaks in $(\varepsilon - \mu)(\partial f(\varepsilon)/\partial \varepsilon)$ go far below and above the hump, respectively. Since the $\sigma(\varepsilon)$ more rapidly decreases with decreasing energy below the hump energy than with increasing energy above the hump energy, $|Q_+(T)|/T$ decreases much more rapidly than $|Q_-(T)|/T$. $S(T)$ at high temperature, thus, decreases with increasing temperature, and eventually turns out to be negative at T_{cross} . In this way, the

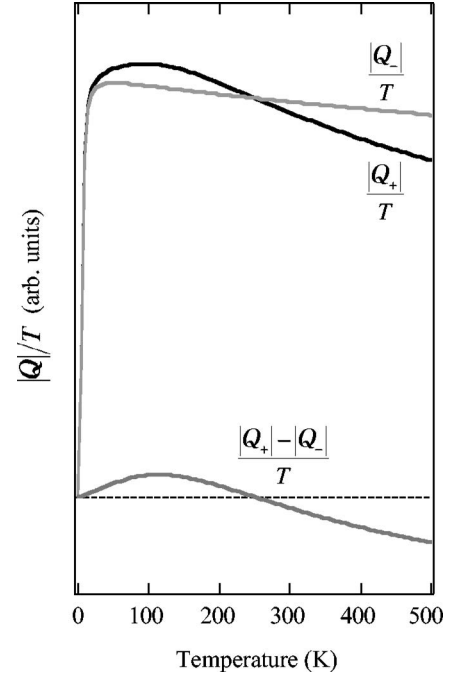


FIG. 7. The magnitude of positive energy flow $|Q_+(T)|$ and that of negative energy flow $|Q_-(T)|$ divided by T , which are carried by the electrons below and above μ , respectively. The $(|Q_+(T)| - |Q_-(T)|) / T$, which mainly determines the magnitude and sign of $S(T)$, is also shown.

characteristic behavior of $S(T)$ is almost completely accounted for.

In order to examine whether our present calculation of $S(T)$ for Bi2201 is universally applicable for other cuprate superconductors, we calculated $S(T)$ in Bi2212 by using the $\varepsilon - \mathbf{k}$ dispersion reported by Norman *et al.*²⁰ The calculated $S(T)$'s for Bi2212 of different doping levels are shown in Fig. 8, together with the measured one with various T_c reported by Munakata *et al.*⁴² The p 's for the calculated $S(T)$'s are estimated from A_{pFS} 's and are shown in the same panel. The calculated $S(T)$'s for the samples with $p=0.17$ and 0.26 holes/Cu, which are considered to be in optimally and overdoped conditions, respectively, quantitatively reproduce the measured $S(T)$'s of the optimally and overdoped samples with $T_c=86$ K and $T_c=76$ K, respectively. The large values exceeding $20 \mu\text{V/K}$, measured for the underdoped samples, cannot be reproduced by the present calculation. These conditions are exactly the same as those for the present Bi2201 samples.

The present calculation of $S(T)$ in Bi2212 were performed without considering the presence of the bilayer splitting in the band structure, which were clearly observed in Bi2212 by the recent high-resolution ARPES measurement.²⁵⁻²⁷ The saddle point producing vHs near μ observed in Norman's band corresponds to that in the antibonding band, while that of the bonding band is located far below μ . Therefore we consider that $S(T)$ of Bi2212 would not be greatly affected by the bonding band, and that is why our calculation of $S(T)$ in Bi2212 on the basis of the band structure reported by Norman *et al.*²⁰ provides us a reasonable result.

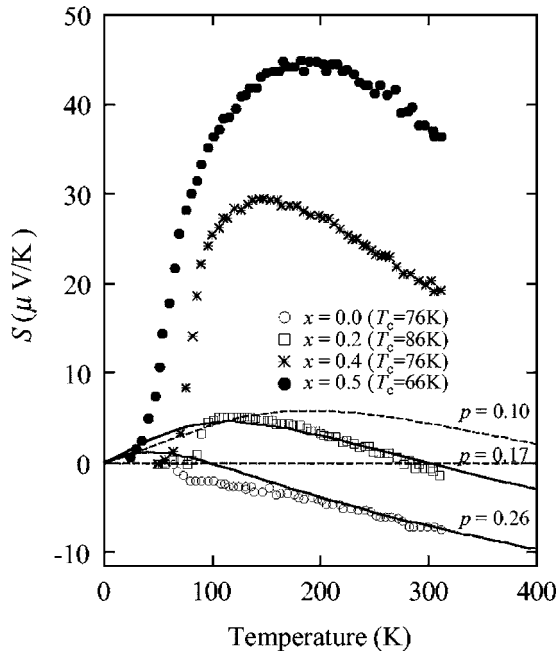


FIG. 8. The measured (Ref. 42) and calculated $S(T)$ of the $\text{Bi}_2\text{Sr}_2\text{Ca}_{1-x}\text{Y}_x\text{Cu}_2\text{O}_{8+\delta}$ (Bi2212). The calculation was performed using the $\varepsilon-\mathbf{k}$ dispersion reported by Norman *et al.* (Ref. 20). The quantitative agreement between the measured and calculated $S(T)$ is observed for the optimally and overdoped samples. The large $S(T)$ exceeding $20 \mu\text{V/K}$ in underdoped samples cannot be reproduced by the present calculation.

We propose here some possible reasons for the unusual behavior of $S(T)$ in the underdoped sample.

The first one is related to the problem in the band determination method we used in this paper. It is reported that the spectra in the underdoped samples are fairly broadened, especially around $(\pi, 0)$, because of the very short lifetime of the Bloch states due to the strong electron correlation.^{43,44} We did not take this effect into account, but simply used the peak energy of the spectrum as the eigenvalue for the selected momentum. If the wave number \mathbf{k} is no longer a good quantum number because of the strong scattering limit, the $\varepsilon-\mathbf{k}$ dispersion determined by the peaks of ARPES spectra cannot be used to evaluate $S(T)$. This may cause inconsistency between the calculated $S(T)$ and measured one, especially in the underdoped samples.

The assumption of a constant mean-free path (l), employed in our analysis, would be inappropriate, especially in the underdoped samples. We found that the MDC width in the present overdoped Bi2201 samples possesses a less significant momentum dependence and moderate energy dependence in the very narrow energy range used in our calculation of $S(T)$. This experimental observation encouraged us to

employ the constant l approximation. It was reported for Bi2212, however, that the ARPES spectra around $(\pi, 0)$ get drastically broadened with decreasing p , especially in the underdoped samples, in sharp contrast to the spectral width at \mathbf{k}_F in the $(0, 0)-(\pi, \pi)$ direction, possessing almost no p dependence.^{43,44} These results suggest that the momentum-dependent scattering events are enhanced in the underdoped condition. If this anisotropy of the scattering events causes a strong energy dependence in l and resulting $\sigma(\varepsilon)$, $S(T)$ would be greatly affected by it.

Another mechanism, which is the most plausible one, should be discussed in terms of a pseudogap. It is well known that the pseudogap persists up to a higher temperature than T_c in the underdoped condition.^{45,46} A temperature- and p -dependent pseudogap would cause strong variation in $\sigma(\varepsilon)$ and resulting $S(T)$. The detailed analysis on $S(T)$ under the pseudogap formation is far beyond our present analysis. Since the effect of the pseudogap cannot be fully understood without a further detailed investigation, we keep this problem open.

Before closing the discussion, we should comment on the empirical use of $S(290 \text{ K})$ for the p estimation proposed by Obertelli *et al.*⁷ This empirical method to estimate p is constructed on the basis of two relations: T_c/T_c^{max} as a function of $S(290 \text{ K})$, and $T_c/T_c^{\text{max}} = 1 - 82.6(p - 0.16)$.² We showed in this paper that both experimental relations of T_c/T_c^{max} vs $S(290 \text{ K})$ and T_c/T_c^{max} vs p are not applicable, at least for the present Bi2201 samples. We found that $S(T)$ is unambiguously determined by the vHs instead of these relations. A fairly large difference in the shape of vHs on $N(\varepsilon)$ between Bi2201 and Bi2212 suggests that the absolute value of p has less important effects on the magnitude of $S(290 \text{ K})$. We conclude, therefore, that $S(290 \text{ K})$ cannot be used to estimate p in the cuprate superconductors.

V. CONCLUSION

The band structure (the $\varepsilon-\mathbf{k}$ dispersion) of Bi2201 with various p 's was determined by ARPES measurements. By using the experimentally determined $\varepsilon-\mathbf{k}$ dispersion, we calculated $S(T)$ within the framework of the Boltzmann transport theory. The calculated $S(T)$ quantitatively reproduced the measured one in the optimally and overdoped samples. It is found, as a consequence of the present analysis, that the temperature and p dependence of $S(T)$ in Bi2201 is well accounted for by considering the presence of the van Hove singularity near the Fermi level and the energy shift of μ with a varying hole concentration. We also found that $S(290 \text{ K})$ cannot be used to estimate p in Bi2201 and other cuprate superconductors.

- ¹J. R. Cooper and J. W. Loram, *J. Phys. I* **6**, 2237 (1996).
- ²Y. Dumont, C. Ayache, and G. Collin, *Phys. Rev. B* **62**, 622 (2000).
- ³V. E. Gasumyants, N. V. Ageev, E. V. Vladimirskaia, V. I. Smirnov, A. V. Kazanskiy, and V. I. Kaydanov, *Phys. Rev. B* **53**, 905 (1996).
- ⁴V. E. Gasumyants, V. I. Kaidanov, and E. V. Vladimirskaia, *Physica C* **248**, 255 (1995).
- ⁵C. K. Subramaniam, C. V. N. Rao, A. B. Kaiser, H. J. Trodahl, A. Mawdsley, N. E. Flower, and J. L. Tallon, *Supercond. Sci. Technol.* **7**, 35 (1994).
- ⁶S. Keshri, J. B. Mandal, P. Mandal, A. Poddar, A. N. Das, and B. Ghosh, *Phys. Rev. B* **47**, 9048 (1993).
- ⁷S. D. Obertelli, J. R. Cooper, and J. L. Tallon, *Phys. Rev. B* **46**, R14928 (1992).
- ⁸M. R. Presland, J. L. Tallon, R. G. Buckley, R. S. Liu, and N. E. Flower, *Physica C* **176**, 95 (1991).
- ⁹M. V. Elizarova and V. E. Gasumyants, *Phys. Rev. B* **62**, 5989 (2000).
- ¹⁰T. Nishikawa, J. Takeda, and M. Sato, *J. Phys. Soc. Jpn.* **63**, 1441 (1994).
- ¹¹Y. Ando, Y. Hanaki, S. Ono, T. Murayama, K. Segawa, N. Miyamoto, and S. Komiya, *Phys. Rev. B* **61**, R14956 (2000).
- ¹²H. J. Trodahl, *Phys. Rev. B* **51**, R6175 (1995).
- ¹³Z. Konstantinovic, G. Le Bras, A. Forget, D. Colson, F. Jean, G. Collin, M. Ocio, and C. Ayache, *Phys. Rev. B* **66**, 020503(R) (2002).
- ¹⁴G. Hildebrand, T. J. Hagenaaers, W. Hanke, S. Grabowski, and J. Schmalian, *Phys. Rev. B* **56**, R4317 (1997).
- ¹⁵K. Durczewski and M. Ausloos, *Phys. Rev. B* **61**, 5303 (2000).
- ¹⁶D. M. Newns, C. C. Tsuei, R. P. Huebener, P. J. M. van Bentum, P. C. Pattnaik, and C. C. Chi, *Phys. Rev. Lett.* **73**, 1695 (1994).
- ¹⁷Yoshimi Kubo, *Phys. Rev. B* **50**, 3181 (1994).
- ¹⁸G. C. McIntosh and A. B. Kaiser, *Phys. Rev. B* **54**, 12569 (1996).
- ¹⁹T. Takeuchi, T. Yokoya, S. Shin, K. Jinno, M. Matsuura, T. Kondo, H. Ikuta, and U. Mizutani, *J. Electron Spectrosc. Relat. Phenom.* **114**, 629 (2001).
- ²⁰M. R. Norman, M. Randeria, H. Ding, and J. C. Campuzano, *Phys. Rev. B* **52**, 615 (1995).
- ²¹T. Sato, H. Matsui, S. Nishina, T. Takahashi, T. Fujii, T. Watanabe, and A. Matsuda, *Phys. Rev. Lett.* **89**, 067005 (2002).
- ²²A. Ino, C. Kim, M. Nakamura, T. Yoshida, T. Mizokawa, A. Fujimori, Z.-X. Shen, T. Kakeshita, H. Eisaki, and S. Uchida, *Phys. Rev. B* **65**, 094504 (2002).
- ²³D. H. Lu, D. L. Feng, N. P. Armitage, K. M. Shen, A. Damascelli, C. Kim, F. Ronning, Z.-X. Shen, D. A. Bonn, R. Liang, W. N. Hardy, A. I. Rykov, and S. Tajima, *Phys. Rev. Lett.* **86**, 4370 (2001).
- ²⁴T. Sato, H. Kumigashira, D. Ionel, T. Takahashi, I. Hase, H. Ding, J. C. Campuzano, and S. Shamoto, *Phys. Rev. B* **64**, 075103 (2001).
- ²⁵D. L. Feng, N. P. Armitage, D. H. Lu, A. Damascelli, J. P. Hu, P. Bogdanov, A. Lanzara, F. Ronning, K. M. Shen, H. Eisaki, C. Kim, and Z.-X. Shen, *Phys. Rev. Lett.* **86**, 5550 (2001).
- ²⁶Y. D. Chuang, A. D. Gromko, A. Fedorov, Y. Aiura, K. Oka, Yoichi Ando, H. Eisaki, S. I. Uchida, and D. S. Dessau, *Phys. Rev. Lett.* **87**, 117002 (2001).
- ²⁷P. V. Bogdanov, A. Lanzara, X. J. Zhou, S. A. Kellar, D. L. Feng, E. D. Lu, H. Eisaki, J.-I. Shimoyama, K. Kishio, Z. Hussain, and Z. X. Shen, *Phys. Rev. B* **64**, 180505(R) (2001).
- ²⁸H. Ding, A. F. Bellman, J. C. Campuzano, M. Randeria, M. R. Norman, T. Yokoya, T. Takahashi, H. Katayama-Yoshida, T. Mochiku, K. Kadowaki, G. Jennings, and G. P. Brivio, *Phys. Rev. Lett.* **76**, 1533 (1996).
- ²⁹H. M. Fretwell, A. Kaminski, J. Mesot, J. C. Campuzano, M. R. Norman, M. Randeria, T. Sato, R. Gatt, T. Takahashi, and K. Kadowaki, *Phys. Rev. Lett.* **84**, 4449 (2000).
- ³⁰J. M. Tarascon, W. R. McKinnon, Y. LePage, K. Remschig, R. Ramesh, R. Jones, G. Pleizier, and G. W. Hull, *Physica C* **172**, 13 (1990).
- ³¹V. Manivannan, J. Gopalakrishnan, and C. N. R. Rao, *Phys. Rev. B* **43**, R8686 (1991).
- ³²I. Chong, T. Terashima, Y. Bando, M. Takano, Y. Matsuda, T. Nagaoka, and K. Kumagai, *Physica C* **290**, 57 (1997).
- ³³Y.-D. Chuang, A. D. Gromko, D. S. Dessau, Y. Aiura, Y. Yamaguchi, K. Oka, A. J. Arko, J. Joyce, H. Eisaki, S. I. Uchida, K. Nakamura, and Yoichi Ando, *Phys. Rev. Lett.* **83**, 3717 (1999).
- ³⁴T. Greber, T. J. Kreuzer, and J. Osterwalder, *Phys. Rev. Lett.* **79**, 4465 (1997).
- ³⁵T. Kondo, T. Takeuchi, T. Yokoya, S. Tsuda, S. Shin, and U. Mizutani, *J. Electron Spectrosc. Relat. Phenom.* **137-140**, 663-668 (2004).
- ³⁶A. Lanzara, P. V. Bogdanov, X. J. Zhou, S. A. Kellar, D. L. Feng, E. D. Lu, T. Yoshida, H. Eisaki, A. Fujimori, K. Kishio, J.-I. Shimoyama, T. Noda, S. Uchida, Z. Hussain, and Z.-X. Shen, *Nature (London)* **412**, 510 (1998).
- ³⁷T. Sato, H. Matsui, T. Takahashi, H. Ding, H.-B. Yang, S.-C. Wang, T. Fujii, T. Watanabe, A. Matsuda, T. Terashima, and K. Kadowaki, *Phys. Rev. Lett.* **91**, 157003 (2003).
- ³⁸H. Takagi, T. Ido, S. Ishibashi, M. Uota, S. Uchida, and Y. Tokura, *Phys. Rev. B* **40**, 2254 (1989).
- ³⁹J. B. Torrance, A. Bezing, A. I. Nazzari, T. C. Huang, S. S. P. Parkin, D. T. Keane, S. J. LaPlaca, P. M. Horn, and G. A. Held, *Phys. Rev. B* **40**, 8872 (1989).
- ⁴⁰H. Ding, M. R. Norman, T. Yokoya, T. Takeuchi, M. Randeria, J. C. Campuzano, T. Takahashi, T. Mochiku, and K. Kadowaki, *Phys. Rev. Lett.* **78**, 2628 (1997).
- ⁴¹T. Valla, A. V. Fedorov, P. D. Johnson, B. O. Wells, S. L. Hulbert, Q. Li, G. D. Gu, and N. Koshizuka, *Science* **285**, 2110 (1999).
- ⁴²F. Munakata, K. Matsuura, K. Kubo, T. Kawano, and H. Yamachi, *Phys. Rev. B* **45**, 10604 (1992).
- ⁴³Z.-X. Shen and J. R. Schrieffer, *Phys. Rev. Lett.* **78**, 1771 (1997).
- ⁴⁴M. R. Norman, H. Ding, M. Randeria, J. C. Campuzano, T. Yokoya, T. Takeuchi, T. Takahashi, T. Mochiku, K. Kadowaki, P. Guptasarma, and D. G. Hinks, *Nature (London)* **392**, 157 (1998).
- ⁴⁵H. Ding, T. Yokoya, J. C. Campuzano, T. Takahashi, M. Randeria, M. R. Norman, T. Mochiku, K. Kadowaki, and J. Giapintzakis, *Nature (London)* **382**, 51 (1996).
- ⁴⁶A. G. Loeser, Z.-X. Shen, D. S. Dessau, D. S. Marshall, C. H. Park, P. Fournier, and A. Kapitulnik, *Science* **273**, 325 (1996).